ACS APPLIED MATERIALS & INTERFACES

www.acsami.org

Research Article

Commercial Janus Fabrics as Reusable Facemask Materials: A Balance of Water Repellency, Filtration Efficiency, Breathability, and Reusability

Steven Cheng, Weixing Hao, Yuchen Wang, Yang Wang, and Shu Yang*

Cite This: *ACS Appl. Mater. Interfaces* 2022, 14, 32579–32589

Read Online

ACCESS | Metrics & More | Article Recommendations | Supporting Information

ABSTRACT: Facemasks as personal protective equipment play a significant role in helping prevent the spread of viruses during the COVID-19 pandemic. A desired reusable fabric facemask should strike a balance of water repellency, good filtration efficiency (FE), breathability, and mechanical robustness against washing cycles. Despite significant efforts in testing various commercial fabric materials for filtration efficiency, few have investigated fabric performance as a function of the fiber/yarn morphology and wettability of the fabric itself. In this study, we examine commercial fabrics with Janus-like behaviors to determine the best reusable fabric facemask materials by understanding the roles of morphology, porosity, and wettability of the fabric on its overall performance. We find that the outer layer of the diaper fabric consisted of laminated polyurethane, which is hydrophobic, has low porosity (~5%) and tightly woven yarn structures, and shows the highest overall FE (up to 54%) in the submicron particle size range (0.03–0.6 μm) among the fabrics tested. Fabric layers with higher porosity lead to lower-pressure drops, indicating higher breathability but lower FE. Tightly woven waterproof rainwear fabrics perform the best after 10 washing cycles, remaining intact morphologically with only a 2–5% drop in the overall FE in the submicron particle size range, whereas other knitted fabric layers become loosened and the laminated polyurethane thin film on the diaper fabric is wrinkled. In comparison, the surgical masks and N95 respirators made from nonwoven polypropylene (PP) fibers see over a 30% decline in the overall FE after 10 washing cycles. Overall, we find that tightly woven Janus fabrics consisting of a low porosity, a hydrophobic outer layer, and a high porosity and hydrophilic inner layer offer the best performance among the fabrics tested as they can generate a high overall FE, achieve good breathability, and maintain fabric morphology and performance over multiple washing cycles.

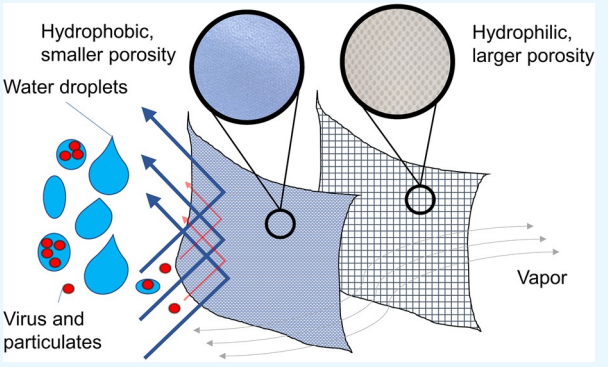

KEYWORDS: *Janus fabrics, filtration efficiency, surface interactions, facemask, reusability*

INTRODUCTION

During the COVID-19 pandemic, wearing facemasks has been a central public health measure to reduce the transmission of the SARS-CoV-2 virus. Surgical masks and N95 respirators have been widely used in the workplace of the healthcare and manufacturing sectors to prevent the spread of water droplets and aerosols, the main carriers of the coronavirus.[1,2] For example, N95 respirators have a >95% particle filtration efficiency (PFE) at a 0.3 micron pore size and a >99% bacterial filtration efficiency (BFE).[3] However, these filters also restrict breathing airflow, making them uncomfortable to wear for a prolonged time, especially in hot weather. Many commonplace filter materials and household fabrics have been investigated for repurposing them into masks.[4−26] Despite significant efforts in testing various commercial fabric materials for high filtration efficiency (FE), there lacks a comprehensive investigation of the fabric performance as a function of the fiber/yarn morphology and wettability to balance the complex requirements of droplet repellency, FE, breathability, and washability for daily-use fabric facemasks.

A desirable fabric facemask should repel aerosols from landing on them, be able to filter out particles to prevent the penetration of viruses, allow airflow from inside through the mask to be breathable, and be durable after multiple washing cycles for reuse. The SARS-CoV-2 viruses have a diameter of 100–300 nm and are mostly found in aerosols and liquid droplets less than 5 μm in size,[4,5] highlighting the need to effectively prevent aerosols and liquid droplets from landing on or penetrating through fabrics. Mechanical filtration mecha-

Received: May 28, 2022
Accepted: June 26, 2022
Published: July 7, 2022

https://doi.org/10.1021/acsami.2c09544
ACS Appl. Mater. Interfaces 2022, 14, 32579–32589

nisms involve diffusion, interception, gravitational settling, and inertial impaction depending on the size of the particles.[27−34] Electrostatic interactions can induce particle trapping on electrically charged fibers, thus further enhancing filtration efficiency (FE) for particles less than 100 nm while using fabrics with pore size greater than 300 nm.[8−10] In general, fabrics consisting of smaller porosity[7,22] and multiple layers[6,7,11,12] will have higher FE, although there is a trade-off between breathability and FE.[7,16,17,30] Meanwhile, the wettability of the fabric's outer surface will determine how well aerosols and droplets will interact with the fabric surface layer and layers in between, such as the capture of wetting droplets on the polyimide nanofibers with a small contact angle.[35] Thus, water repellency of the outer surface is highly desired. Facemasks must also be breathable to maximize comfort when worn on the body and allow for the transmission and diffusion of moisture and CO_2 vapor away from the face.[7] To minimize waste from disposable masks, which are not recyclable, reusable fabric masks that can maintain their structural integrity and nonwettability after each washing cycle will be preferred. It is known that melt-spun, nonwoven surgical and N95 masks will deteriorate after washing.[19] The World Health Organization (WHO) recommends that fabric masks worn are made of three layers of fabric: an inner layer of absorbent material, a middle layer of nonwoven nonabsorbent material, and an outer layer of nonabsorbent material.[36] Yet, little is known about the role of the fabric's knitting or weaving structures on performance after washing.

Commercial fabrics, especially those used for rainwear, athletic wear, and diaper wear, are of great interest in this study. Rainwear materials are commonly made from polymers that offer durable water repellency and breathability, e.g., poly(tetrafluoroethylene) (PTFE) that have microporous structures to prevent the penetration of water from outside while allowing for vapor molecules to evaporate across the micropores.[37,38] Rain jackets come in 2-, 2.5-, and 3-layer variations. The one that has a durable water repellency coating on the face layer and a waterproof inner layer is referred to as the 2-layer fabric. When a half-layer is printed or sprayed with materials on the inside of the jacket, usually in a pattern such as dots or lines, which have different contrasts from the face layer and the inner layer, it is referred to as the 2.5-layer fabric. The 3-layer fabric has a water repellency face layer, a waterproof membrane middle layer, and a pressed high-performance inner liner designed to be breathable while protecting the middle membrane from oils and dirt. Likewise, athletic wears are known for their moisture-wicking behaviors, where sweat vapor is drawn from the inner layer in contact with the body, which is typically hydrophilic such as cotton via capillary action and transported toward the outer layer, which is more hydrophobic such as polyester.[39,40] Cloth diaper often has a woven inner layer that is hydrophilic and soft to the skin touch, a middle layer that is water-absorbing, and an outer layer consisting of a laminated polyurethane (PU) film that repels moisture from the outside and prevents leakage from inside.[41] These functional fabric materials all share common functions, which are to keep the body dry, to remain breathable and comfortable to wear for an extended time, and to efficiently transport vapor from the body. These fabric materials are Janus in nature with multilayered structures. For fabric facemasks, it will be desired to have a hydrophobic outer layer to repel the aerosols and a hydrophilic inner layer facing the nose and mouth to bring breath away.[42−46] Here, we examine several commercial fabric materials of Janus nature in terms of the fabric morphology, specifically the weaving or knitting fiber or yarn diameter, pattern, and pore size, where the surface characteristics are different in the outer and inner layers. We characterize the FE performance, wettability, and reusability of the fabrics. Understanding these relationships will offer insights into the design of fabric facemasks with improved filtration efficiency and reusability while maintaining comfort and breathability.

EXPERIMENTAL METHODS

Commercial Fabrics Tested. Sample 1: a 3-layer laminate poly twill with ePTFE film 100% Poly Unbrushed Tricot—Medical Green (RockyWoods). Sample 2: WeatherTek 2.5-layer ePTFE waterproof breathable ripstop nylon fabric (Spirit West). Samples 3 and 4: hydrophilic (sample 3) and hydrophobic (sample 4) polyesters, which are thermally laminated with a layer of thermoplastic polyurethane (TPU) film (Kinderel Organic Fabrics), often referred to as polyurethane laminate (PUL) and are commonly used in fabric diapers. 3-ply surgical masks (Ecoparks; Walgreens), N95 respirators (Model 8210, 3M, and SDELC), and KN95 respirators (NIDI, China and JINJIANG, China) are also tested.

Characterization of Fabrics. Each side of the 1 inch x 1 inch fabric sample was examined under an Olympus 7500 optical microscope in reflection and transmission modes. Scanning electron microscopy (SEM) images were taken on 1 cm × 1 cm fabric samples on an FEI Quanta 600 FEG ESEM in an environmental mode at 5 keV. Yarn spacing, yarn diameter, yarn width, and fabric thickness were obtained with 100-line measurements using ImageJ software (National Institute of Health). The porosity and thread count density were estimated from the SEM images. A goniometer (Ramé-Hart, Model 200) was used to obtain the static and dynamic water contact angles and contact angle hysteresis from each side of the Janus fabrics using the sessile drop method and averaged from the measurement of five fresh spots.

Evaluation of the Filtration Efficiency and Breathing Resistance of Fabrics. The experimental setup to evaluate the filtration efficiency and breathing resistance of fabrics can be found in Figure S1 in the Supporting Information. The procedure and method used are similar to those reported in our previous studies.[11,12] The test aerosols were generated by a constant output atomizer (Model 3076, TSI Inc.), nebulizing a NaCl−water solution with a mass concentration of 0.1%. The atomizer generated aerosols at a flow rate of 3.0 liter per minute (lpm). The aerosols were first diluted by an inline diluter and then dried by a homemade diffusion dryer. Afterward, the aerosols, together with a stream of filtered make-up air, were introduced into a mixing chamber. To control the relative humidity (RH) of the make-up air and hence the RH of the mixed aerosol flow, the make-up air was introduced into a fritted glass water bubbler (Thomas Scientific, Swedesboro, NJ). To remove the suspended droplets, the humidified make-up air was introduced into an inline filter (HEPA Capsule, Pall Inc., Show Low, AZ) before mixing with the aerosol flow. Therefore, the relative humidity of the mixed aerosol flow was determined by the temperature of the water bubbler and measured by an RH sensor (Model GPS-6, Elitech Inc., San Jose, CA). The conditioned aerosols were then directed into a filter holder (Air Sampling Cassette, Zefon International Inc.), where the disc-shaped filter material, here the cut fabric with a diameter of 37 mm, was firmly pressed onto mesh support and sealed at the edge.

The flow rate through a filter is varied by the face velocity. Given the variabilities of breathing flow rates depending on the age, gender, and motion status of a person, common filter materials have been tested under a wide range of face velocities, ranging from 5.3 to 26 cm s^{-1}.[47−50] In this study, we examined the filtration performance of the fabric materials under a face velocity of 9.2 cm s^{-1}, corresponding to a flow rate of 6 lpm through the 37 mm sampling cassette. Measurements of filtration performance were conducted at a face velocity of 5.3 cm s^{-1} (NIOSH Procedure No. TEB-APR-STP-0059, 2019), and the results can be found in the Supporting Information.

https://doi.org/10.1021/acsami.2c09544
ACS Appl. Mater. Interfaces 2022, 14, 32579−32589

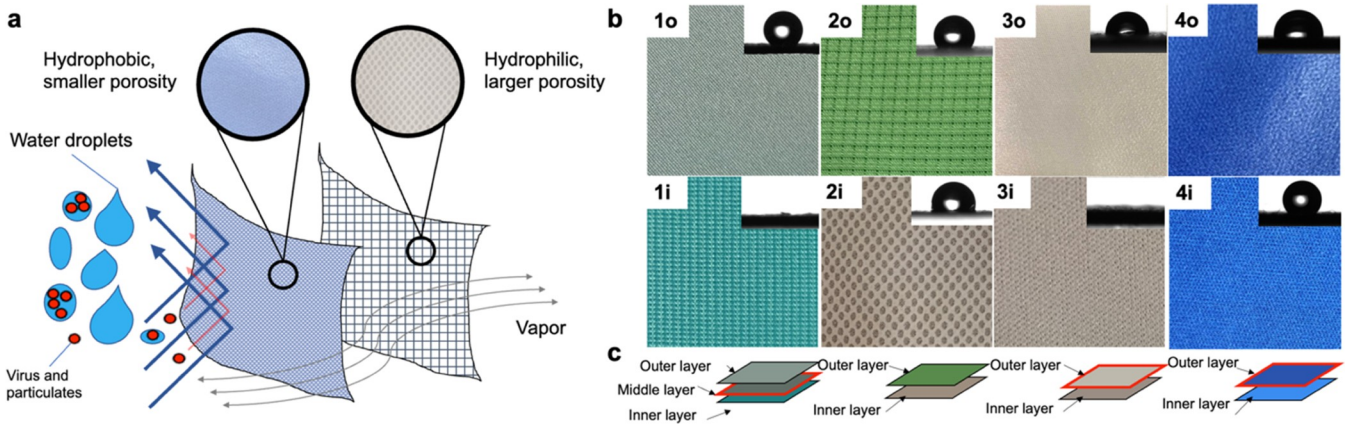

Figure 1. (a) Schematic of the preferred Janus fabrics with layered structures. (b) Images of the outer layer (o) and the inner layer (i) of different Janus fabrics. Inset: optical images of a 5 μL water droplet sitting on the fabric surface. Sample 1: a 3-layer laminate poly twill fabric with a middle ePTFE film. Sample 2: a 2.5-layer waterproof breathable ripstop fabric. Sample 3: a thermally laminated TPU fabric with a hydrophilic inner layer. Sample 4: a thermally laminated TPU fabric with a hydrophobic inner layer. (c) Illustrations of the cross-sectional views of the fabrics. The outlined layer represents the film layer.

The effect of using a range of face velocities on filtration performance can be found in an earlier study.[11] A scanning mobility particle sizer (SMPS, Model 3936, TSI Inc.) measured the mobility size distributions of aerosols upstream and downstream of the filter holder. The SMPS system was equipped with a differential mobility analyzer (DMA, Model 3081, TSI Inc.) that classified particles in the range between 10 and 600 nm and a condensation particle counter (CPC, Model 3750) that measured the concentration of the mobility-classified particles. As the flow resistance across the filter material is a critical component in assessing the breathability of the material, a digital manometer (RISEPRO, 365BG947677, measuring range ±13.79 kPa, 0.001 kPa resolution) was used to monitor the flow resistance of the materials.

Evaluation of the Impact of Washing. To evaluate the impact of washing, each fabric sample underwent multiple washing cycles, each for 30 min under a cold rinse cycle in a commercial washing machine (Model # FWS933FS, Frigidaire). The fabric samples were then hanged and left to air-dry. After each washing cycle, the morphology, water contact angles, filtration efficiency, and breathing resistance of each sample were characterized.

RESULTS AND DISCUSSION

An ideal material for making fabric facemasks should have water repellency and high FE performance to filter out virus-containing aerosols, high breathability for maximal user comfort, and mechanical robustness for reusability. Previous studies on facemask materials mainly focus on repurposing them to address the facemask shortage. Therefore, filtration performance is the highest priority in selecting materials for evaluation, whether household fabrics or commercial filters. The filtration efficiency and breathability of common household fabric materials, such as cotton T-shirts, bandanas, linen, silk, pillowcases, and paper towels, whether single-layered or multilayered, have been widely studied.[6,11,12,21] The overall filtration efficiencies are typically <25%, generating a flow resistance of up to 5 kPa, at least 10 times higher than those from nonwoven surgical masks and N95 respirators.[9] Commercial filter materials such as coffee filters, HVAC household air filters, and vacuum bags have also been evaluated, showing an overall FE performance of up to 80% while generating a flow resistance of around 0.5 kPa, similar to those of surgical masks and N95 respirators.[11,12] It has been well established that there is a trade-off between the overall FE and breathability,[9,16,17,30] necessitating the question of how different fabric characteristics in different layers may contribute to optimizing both properties. While some studies provide information such as surface wettability or fabric morphology,[8,11,12,18,26,30] few have evaluated the washability of these fabrics.[15] Taken together, it remains to be addressed how the different characteristics in fabric materials will contribute to the overall performance of the fabric facemasks, including the overall water repellency, FE, breathability, and durability against repeated machine washing. Here, we select and evaluate four commercial Janus-like fabrics that have contrasting material characteristics between the inner and outer layers of the fabrics.

Structural and Wetting Influence on Filtration Efficiency and Breathability of Fabrics. As seen in Figure 1a, the inner layer and outer layer of the fabric materials have different weaving pattern densities and wetting characteristics. For homemade facemask use, preferably, the outer layer should repel water droplets and aerosols containing viruses as the first line of defense. Thus, it should be more hydrophobic and have a lower air porosity that will offer higher FE against small particles (≤300 nm in size), while the inner layer should be hydrophilic and have a higher air volume fraction or porosity to promote breathability, allowing facile liquid and vapor transport away from a person's breath through capillary action. The fabric morphology is characterized by how the fibers are assembled in woven, knitted, or nonwoven nature, the fiber diameter, the pore size and porosity of the fabric, and the thread count, a standard measurement for the fiber density. Woven fabrics, knitted fabrics, and nonwoven fabrics differ in the interlocking mechanism of the fibers. The mechanical properties of woven and knitted fabrics are highly influenced by structural factors, such as the tension of the stitch, stitch length, and stitch density, and knitted patterns are subject to more deformation than woven patterns when stretched.[51,52] The wetting behavior of the fabric layers is measured by the apparent contact angle (θ^*) of a water droplet on the surface, as a function of Young's contact angle θ on a smooth surface.[53] A surface is considered to be hydrophilic if $\theta < 90°$, and a surface is considered hydrophobic if $90° < \theta < 180°$. θ^* can be significantly increased on a rough surface, described by the Wenzel model, where the liquid is pinned completely to the valleys of the rough surface[54,55]

https://doi.org/10.1021/acsami.2c09544
ACS Appl. Mater. Interfaces 2022, 14, 32579−32589

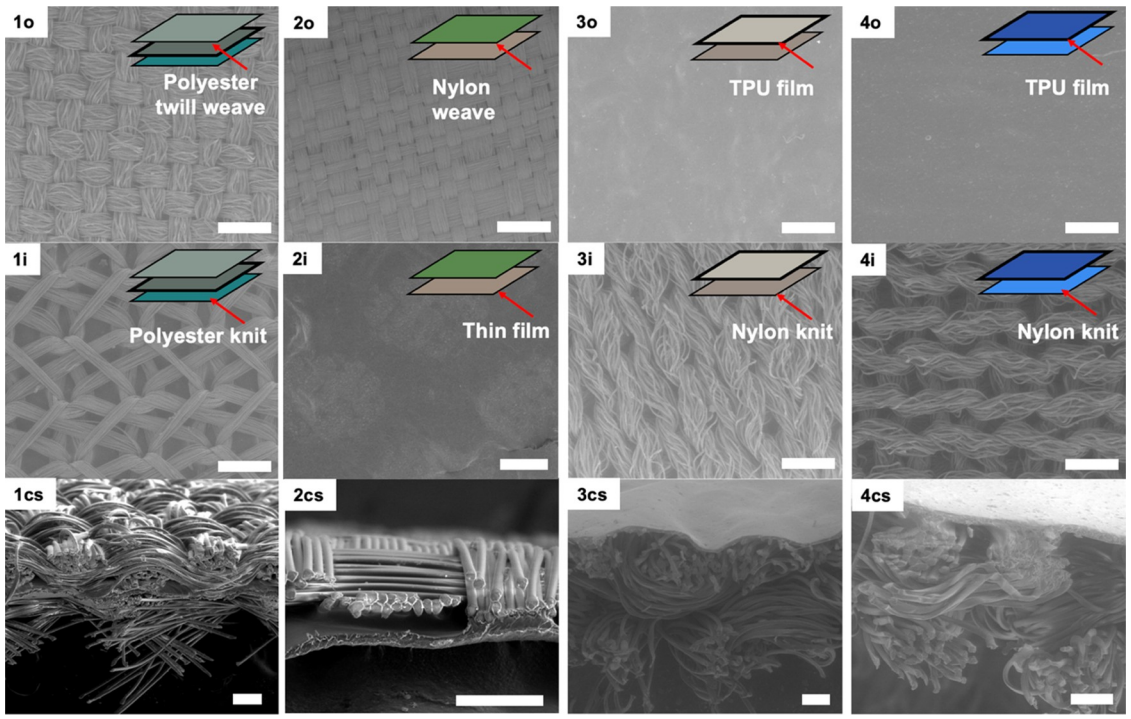

Figure 2. SEM images of the Janus fabrics were investigated. Sample 1: a 3-layer laminate poly twill fabric with a middle ePTFE film. Sample 2: a 2.5-layer waterproof breathable ripstop fabric. Sample 3: a thermally laminated TPU fabric with a hydrophilic inner layer. Sample 4: a thermally laminated TPU fabric with a hydrophobic inner layer. The first row (o) shows the outer layer, the second row (i) shows the inner layer, and the third row (cs) shows the cross-sectional view of the fabrics with the inner layer on top and the outer layer at the bottom. The arrow points to the film layer in each fabric. Scale bars for (o, i) panels: 500 μm, and for (cs) panel: 100 μm.

$$\cos\theta^* = r\cos\theta \quad (1)$$

where r is the surface roughness, defined by the total surface area of the structures divided by the projected surface area. When the liquid sits on a composite surface of air and solid, θ^* is expressed by the Cassie−Baxter model as[56]

$$\cos\theta^* = f_{SL}(\cos\theta + 1) - 1 \quad (2)$$

where f_{SL} is the solid fraction of the rough surface in contact with the liquid.

Another measure to evaluate the wettability of a surface is the contact angle hysteresis (CAH = $\theta_a - \theta_r$), where θ_a is the advancing contact angle, and θ_r is the receding contact angle of a liquid droplet moving on the surface. A lower CAH value indicates a higher mobility of the water droplet on the surface and is less likely to imbibe into the grooves of the rough surface, which is preferred for water repellency. A superhydrophobic surface that repels water is often referred to a surface in the Cassie−Baxter nonwetting state with $\theta^* > 150°$ and CAH less than 10°. Fabrics are porous, which naturally have some degrees of surface roughness. Outer layers with high porosity will be preferred to repel aerosol droplets from penetrating the surface.

The optical images of the outer and inner layers of the four fabrics are shown in Figure 1b. Surgical masks and N95 respirators with multilayered hydrophobic, nonwoven PP fibers are also investigated to highlight the difference in morphology for the comparison of FE and breathability with those of the commercial fabrics studied. Samples 1 and 2, commonly used in water-repellent jackets, were chosen to highlight how the weaving patterns across different layers within a fabric influence their physical properties. Sample 1 is 400 μm thick with a 3-layer laminate poly twill. According to the vendor, it has an expanded poly(tetrafluoroethylene) (ePTFE) middle membrane layer sandwiched between an outer layer of polyester strands in a diagonal twill woven pattern (**1o**) and an inner layer of polyester knits (**1i**), which are tough and durable, and commonly used in linings of snow jackets. ePTFE fibers are commonly used in Gore-Tex known for their waterproof and breathable characteristics, and the expanded fibers provide high mechanical strength and robustness. The outer layer is hydrophobic (θ^* = 142 ± 3°, CAH = 17.9°), consisting of 16.5 μm thick fibers in a 214 ± 19 μm thick yarn, whereas the inner layer is hydrophilic (θ^* = 0°), which has a warp knit pattern with 12 ± 1.5 μm thick fibers. Sample 2 is an 80 μm thick 2.5-layer nylon waterproof breathable ripstop fabric that is commonly used in light rain jackets. It has a hydrophobic (θ^* = 108 ± 7°, CAH = 27.9°) outer layer of woven nylon (**2o**) with 30 μm thick woven fibers (11 ± 1 μm in diameter) spaced 5 μm apart and a hydrophobic (θ^* = 108 ± 7°, CAH = 27.9°) inner layer of a printed film (**2i**), which is often TPU, although the vendor did not specify here. The inner layer and outer layer are bonded together by a thin layer of adhesive. Since no fluorine was detected from either the outer or the inner layer of samples 1 and 2 from our measurement (see the Results and Discussion section), we believe that ePTFE is the middle or the half-layer. Samples 3 and 4 are commonly used in baby diapers and waterproof beddings for stretchability, snug fit, and skin comfort. They are both ∼500 μm thick with an outer layer composed of a 40 μm thick, relatively hydrophobic (θ^* = 94 ± 2°, CAH = 15.4°) TPU film (**3o**, **4o**) thermally laminated on the inner layer of woven nylon (**3i**, **4i**), which is approximately 220 μm thick with 37 μm thick fibers. The inner layer of sample 3 is

https://doi.org/10.1021/acsami.2c09544
ACS Appl. Mater. Interfaces 2022, 14, 32579−32589

Table 1. Information of Surgical Masks, N95 Respirators, and Janus-like Fabric Samples, Including the Filtration Efficiency (FE) at 0.3 μm, Yarn Spacing, Fiber Diameter, Yarn Width, and, When Applicable, Fabric Thickness[a]

sample	FE at 0.3 μm (%)[a]	yarn spacing (μm)	fiber diameter (μm)	yarn width (μm)	fabric thickness (μm)
1i (polyester knit)	48.99 ± 1.61	~500	12.1 ± 1.5	128 ± 18	~400
1o (polyester twill weave)	31.23 ± 0.47	~300	16.5 ± 2.7	214 ± 19	
2i (ePTFE film)	N/A	N/A	N/A	N/A	~80
2o (nylon weave)	N/A	~220	11.1 ± 1	114 ± 22	
3i (nylon knit)	N/A	N/A	37.4 ± 5.1	225 ± 38	~550
3o (TPU film)	63.26 ± 1.26	N/A	N/A	N/A	
4i (nylon knit)	N/A	N/A	17.9 ± 1.9	219 ± 20	~500
4o (TPU film)	53.34 ± 1.53	N/A	N/A	N/A	
5 (surgical mask)	50.07 ± 0.18	N/A	28.4 ± 1.5	N/A	N/A
6 (N95 respirator)	98.16 ± 0.69	N/A	20.1 ± 1.0	N/A	N/A

[a]Some FE data is not available (N/A) because the pressure difference generated at the interface is greater than the maximum value allowed by the SMPS.

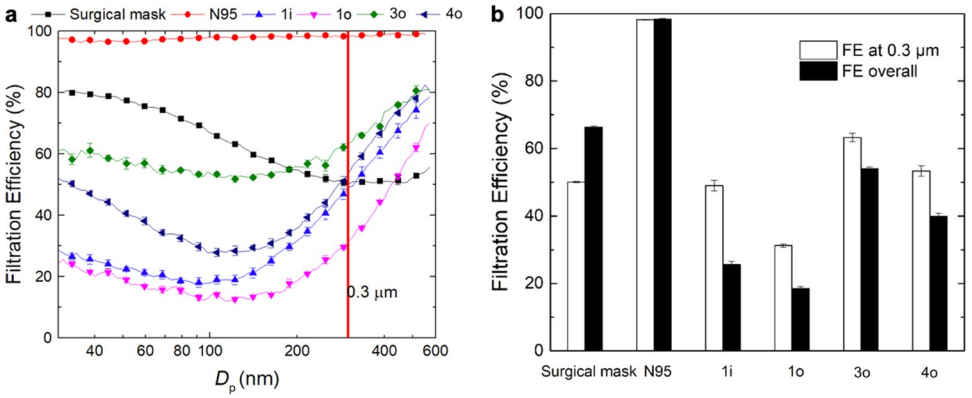

Figure 3. FE of the surgical masks, N95 respirators, and Janus fabric samples obtained at a velocity of 9.2 cm s^{-1}. (a) FE data over a range of submicron particle sizes for the measured samples. (b) Overall FE and FE of 0.3 μm particles. FE data was not obtained for some samples due to a large pressure drop exceeding the maximum value allowed by the SMPS.

hydrophilic ($\theta^* = 0°$), whereas that of sample 4 is hydrophobic ($\theta^* = 130 \pm 3°$, CAH = 18.4°; see the inset of Figure 1b). Top-view and cross-sectional view SEM images were taken from each layer to reveal the Janus nature of the fabrics (see Figure 2). Although the outer layers of all samples are not superhydrophobic, the large θ^* and relatively small CAH (<25°) suggest that they are in between the Cassie and Wenzel states and that aerosols will be less likely to land on the fabric surface. The low porosity of the TPU film in the outer layer of samples 3 and 4 suggests a high overall FE, where particles will be less likely to penetrate through. Since the outer layers of samples 1 and 2 have a higher θ^* and a lower CAH than the outer layers of samples 3 and 4, we expect that they have better water repellency. The nonwoven surgical mask consists of randomly oriented 28.4 ± 1.5 μm fibers, and the N95 respirator consists of randomly oriented 20.1 ± 1.0 μm fibers (Figure S2). It has been suggested that randomly oriented fibers would allow for increased airflow with lower air resistance[7] while efficiently capturing the particles smaller than the pore size. A summary of the layer measurements of each sample is found in Table 1.

The FE of the fabrics can be quantified for a given particle size by measuring the number of particles directed at the fabric (N_U) relative to the number of particles detected after passing through it (N_D)[27−29,57]

$$\mathrm{FE} = 1 - \frac{N_U}{N_D} = 1 - \exp\left(\frac{-4E_f \alpha L}{\pi D_f}\right) \quad (3)$$

FE is proportional to the thickness of the fabric (L) and the fiber filtration efficiency (E_f), a sum of efficiency contributions from mechanical and electrostatic mechanisms, and inversely proportional to porosity (α) and fiber diameter (D_f). Mechanical filtration mechanisms include diffusion, interception, gravitational settling, and impaction.[27,29,58] Since viruses are commonly spread through aerosol droplets, ranging anywhere from 0.3 μm to over 3 μm in size, we investigate the filtration efficiency over a range of particle sizes. Among the size range, the 0.3 μm particle size is essential for evaluating FE because it is the most penetrating particle size (MPPS) range. At the 0.3 μm particle size, the diffusion and inertial impaction mechanical filtration mechanisms overlap, creating a so-called "escape window" where particles can pass through. Evaluating the FE performance at this range is critical to understanding the overall FE performance of a material. The pressure drop (ΔP) across a fabric material can also be related to the physical properties of the fabric:

$$\Delta P = \frac{cLU\eta}{D_f^2} \quad (4)$$

where U is the face velocity, η is the gas viscosity, and c is an arbitrary constant. The pressure drop measures the airflow resistance generated and is a common measure used to determine the breathability of the fabric material. Across multiple layers, FE is multiplicative as particles get filtered out layer by layer. The pressure difference, on the other hand, is additive, suggesting that with the additional layers in a fabric,

https://doi.org/10.1021/acsami.2c09544
ACS Appl. Mater. Interfaces 2022, 14, 32579−32589

Table 2. Filtration Efficiency (FE) and Contact Angle (CA) Information of Surgical Masks, N95 Respirators, and Janus Fabric Samples[a]

sample	FE at 0.3 μm[a] (%)	FE overall (%)	pressure drop (kPa)	static CA (°)	θ_{adv} (°)	θ_{rec} (°)	CAH (°)
1i (polyester knit)	48.99 ± 1.61	25.64 ± 0.99	3.26 ± 0.8	0	N/A	N/A	N/A
1o (polyester twill weave)	31.23 ± 0.47	18.54 ± 0.60	2.95 ± 0.8	142 ± 3	142.4	124.8	17.6
2i (ePTFE film)	N/A	N/A	N/A	108 ± 7	110.8	92.9	27.9
2o (nylon weave)	N/A	N/A	N/A	140 ± 3	150.1	125.4	24.7
3i (nylon knit)	N/A	N/A	N/A	0	N/A	N/A	N/A
3o (TPU film)	63.26 ± 1.26	54.0 ± 0.48	1.71 ± 0.4	94 ± 2	104.4	89.0	15.4
4i (nylon knit)	N/A	N/A	N/A	130 ± 3	137.2	118.8	18.4
4o (TPU film)	53.34 ± 1.53	40.0 ± 0.72	1.91 ± 0.4	97 ± 2	108.6	77.5	31.1
5 (surgical mask)	50.07 ± 0.18	66.37 ± 0.33	0.09 ± 0.01	134 ± 4	129.9	124.5	5.4
6 (N95 respirator)	98.16 ± 0.69	98.37 ± 0.15	0.14 ± 0.02	127 ± 8	140.2	126.6	13.6

[a]Some FE data is not available (N/A) because the pressure difference generated at the interface is greater than the maximum value allowed by the SMPS.

the decrease in breathability gained in increased pressure difference may outweigh the improvement in FE.

We next examine the overall FE performance, size-dependent FE performance, and the pressure drop generated over a range of 0.03−0.6 μm particle sizes at a face velocity of 9.2 cm s^{-1} for the Janus fabrics and compare the performance against the standard surgical masks and N95 respirators since aerosols and droplets of different sizes can carry a range of virus particles (see Figure 3a and Table 2). The comparison between different brands of standard commercial surgical masks, N95, and KN95 respirators is shown in Figure S3. The variation of FE is within 5%, which is not unexpected due to the compliance with the commercial standard. Measurements under a face velocity of 5.3 cm^{-1} can also be found in Table S1 and Figure S4, and no significant influence on FE is observed. We note that FE data was collected only for fabric layers with a low enough pressure drop flow resistance, while FE data for some fabric layers was not accessible because the pressure difference generated at the interface should exceed the maximum value allowed by the SMPS. Here, FE data of the inner and outer layers of sample 1 and the outer layers in samples 3 and 4 were obtained. The weft knit morphology in the **3i** and **4i** layers, although having a relatively higher porosity than those of the woven layers in **1o** and **2o**, generated a larger pressure difference due to the higher amorphous nature of the fibers in the knitting pattern compared to the woven patterns, disrupting airflow and creating air pockets of pressure between the knitting patterns. The thin thickness (80 μm) of sample 2 compared with those of other Janus fabrics tested (400−550 μm) made sample 2 more pliable and susceptible to deform at higher flow velocities, resulting in a much higher pressure flow across the fabric face. Thus, FE was not obtained from sample 2 due to the significant large pressure difference. The overall FE over a range of submicron particle sizes and FE at a 0.3 μm particle size of sample 1 measured from the outer layer are lower than those measured from the inner layer: overall FE of 18.54 ± 0.60% (**1o**) vs 25.64 ± 0.99% (**1i**), FE at 0.3 μm of 31.23 ± 0.47% (**1o**) vs 48.99 ± 1.61% (**1i**), consistent with the fiber morphologies in different layers. In the case of samples 3 and 4, the overall FE performance and FE at 0.3 μm measured from the outer layers are larger than those of **1o**: the overall FE is 54.0 ± 0.48% (**3o**) and 40.0 ± 0.72% (**4o**), and FE at 0.3 μm is 63.26 ± 1.26% (**3o**) and 53.34 ± 1.53% (**4o**). The FE curves of all of the Janus fabric layers show characteristic dips at the MPPS around 100−200 nm (Figure 3a). Here, since the fabrics are not electrostatically charged like the surgical masks and N95 respirators, FE will be highly dependent on pore size and porosity. Thus, smaller particles in the range of sub-0.3 μm can penetrate through the pores between the fabric fibers easily. The nonporous nature of the TPU film at the outer layer of samples 3 and 4, however, allows the interception of smaller particles more readily, leading to a higher FE compared to the woven and knitted layers in sample 1. Comparatively, the presence of electrostatic charges in the middle layers of the nonwoven surgical masks and N95 respirators greatly enhances the interception of particles, thus boosting the FE of the surgical masks (66.37 ± 0.33% overall FE, 50.07 ± 0.18% FE at 0.3 μm) and N95 respirators (98.37 ± 0.15% overall FE, 98.16 ± 0.69% FE at 0.3 μm), despite having a larger porosity in the fiber layers, as shown in Figure S2. We note that the **3o** layer has an FE comparable with surgical masks despite the higher pressure drop (1.71 vs 0.14 kPa, respectively) due to the larger airflow resistance from the nonporous TPU film side.

We subjected the samples to wet aerosols at variable relative humidities (RHs), 20, 40, and 60%, at a face velocity of 9.2 cm s^{-1}. FE at the submicron particle size range remained unchanged as RH increased. At 20% RH, FE at 0.3 μm was 31.23 ± 0.47% (**1o**), 48.99 ± 1.61% (**1i**), 63.26 ± 1.26% (**3o**), and 53.34 ± 1.53% (**4o**). At 60% RH, the average overall FE was 30.52 ± 2.18% (**1o**), 49.20 ± 1.34% (**1i**), 65.68 ± 1.61% (**3o**), and 56.58 ± 0.42% (**4o**) (see the summary in Table 3 and Figure S5). Despite the differences in the wetting behavior between the hydrophilic **1i** sample and the more hydrophobic **1o**, **3o**, and **4o** samples, FE is statistically unchanged with increasing wet aerosol vapor (Figure S5), suggesting that at low and high RH, the mechanical filtration mechanisms are dominant.

The pressure drop of **3o** (ΔP = 1.71 ± 0.4 kPa) and **4o** (ΔP = 1.91 ± 0.4 kPa) is lower than that of **1o** (ΔP = 2.95 ± 0.8 kPa) and **1i** (ΔP = 3.26 ± 0.8 kPa). This can be explained by the morphology of the weave, knit, and film layers, where the film layers with nanopores will have lesser turbulent airflow, compared to the woven layers and knitted layers. Since knitted fabrics have larger air pockets than those between the woven yarns, there may be more interrupted air flows between the bundled yarns. Hence, a higher pressure drop was observed in **1i** of knit patterns (ΔP = 3.26 ± 0.8 kPa) than that in **1o** of woven patterns (ΔP = 2.95 ± 0.8 kPa). In comparison, the pressure drop of the nonwoven surgical mask (ΔP = 0.09 ± 0.01 kPa) and the N95 respirator (ΔP = 0.14 ± 0.02 kPa) is much lower, which has high porosity but randomly oriented

https://doi.org/10.1021/acsami.2c09544
ACS Appl. Mater. Interfaces 2022, 14, 32579−32589

Table 3. FE at 0.3 μm of the Surgical Mask, N95 Respirator, and Janus Fabric Samples Exposed to Various Wet Aerosols at Different Relative Humidities (RHs) at a Face Velocity of 9.2 cm s^{-1}[a]

sample	original RH = 20% (%)	wet aerosol RH = 40% (%)	Wet aerosol RH = 60% (%)
1i (polyester knit)	48.99 ± 1.61	50.21 ± 2.13	49.20 ± 1.34
1o (polyester twill weave)	31.23± 0.47	29.19 ± 1.98	30.52 ± 2.18
2i (ePTFE film)	N/A	N/A	N/A
2o (nylon weave)	N/A	N/A	N/A
3i (nylon knit)	N/A	N/A	N/A
3o (TPU film)	63.26 ± 1.26	64.67 ± 2.21	65.68 ± 1.61
4i (nylon knit)	N/A	N/A	N/A
4o (TPU film)	53.34 ± 1.53	53.04 ± 1.38	56.58 ± 0.42
5 (surgical mask)	50.07 ± 0.18	51.27 ± 0.97	53.45 ± 3.34
6 (N95 respirator)	98.16 ± 0.69	97.71 ± 0.51	97.58 ± 0.37

[a]Some FE data is not available (N/A) because the pressure difference generated at the interface is greater than the maximum value allowed by the SMPS.

fibers (20−25 μm in diameter), thus minimizing air turbulence between the layer. To maximize the breathability of the fabric facemasks, low-pressure drops are desired. Therefore, fabrics with high porosity but less ordered yarns or fibers facing the mouth are preferred for better breathability. The guidance in the porosity for higher breathability conflicts with the characteristics for high FE if electrostatic interactions do not play a role in FE.[7,16,17,30] A hydrophobic surface that limits liquid and aerosol penetration through the fabric can also contribute to FE performance without sacrificing breathability and decreasing fabric porosity.

Role of Wetting and Washing on Filtration Efficiency and Breathability of Fabrics. The reusability of fabric facemasks is essential to minimize waste. Here, the durability of the Janus fabrics was tested against mechanical abrasion during machine washing cycles. Fabrics are cleaned by removing the filtrated particles within. SEM micrographs were taken after five washing cycles, as shown in Figure 4. Wrinkling was seen on the film layers of **2i** and **3o** due to uneven swelling and shrinkage of the fabric layers during the washing and air drying cycles. The film layers were completely wetted during washing. The film layers of **3o** and **2i**, respectively, exhibited larger shrinkage than the more elastic and flexible nylon knits and weaves, where the thermal lamination constrained the film and the yarn layers. Loosened fibers were observed after washing and drying in **3i** and **4i** with nylon woven layers and in the nonwoven surgical mask and N95 respirator layers (seen in Figure S2). In the woven fabrics, the fibers and yarns are physically intertwined; therefore, they are more susceptible to wear and tear by the external forces, whereas yarns are looped and interlocked together in the knitted fabrics, making them highly stretchable. Delamination also occurred in sample 2 with increased fiber/yarn separation in the cross sections of the sample (seen Figure 4). After five washing cycles, there were no significant changes in the morphology of the fabric layers, nor porosity or fabric thickness. Sample 1 remained the most intact morphologically among all of the fabrics.

Mechanical abrasion and damage of the chemical coatings on the fabrics after multiple cycles of washing, however, altered

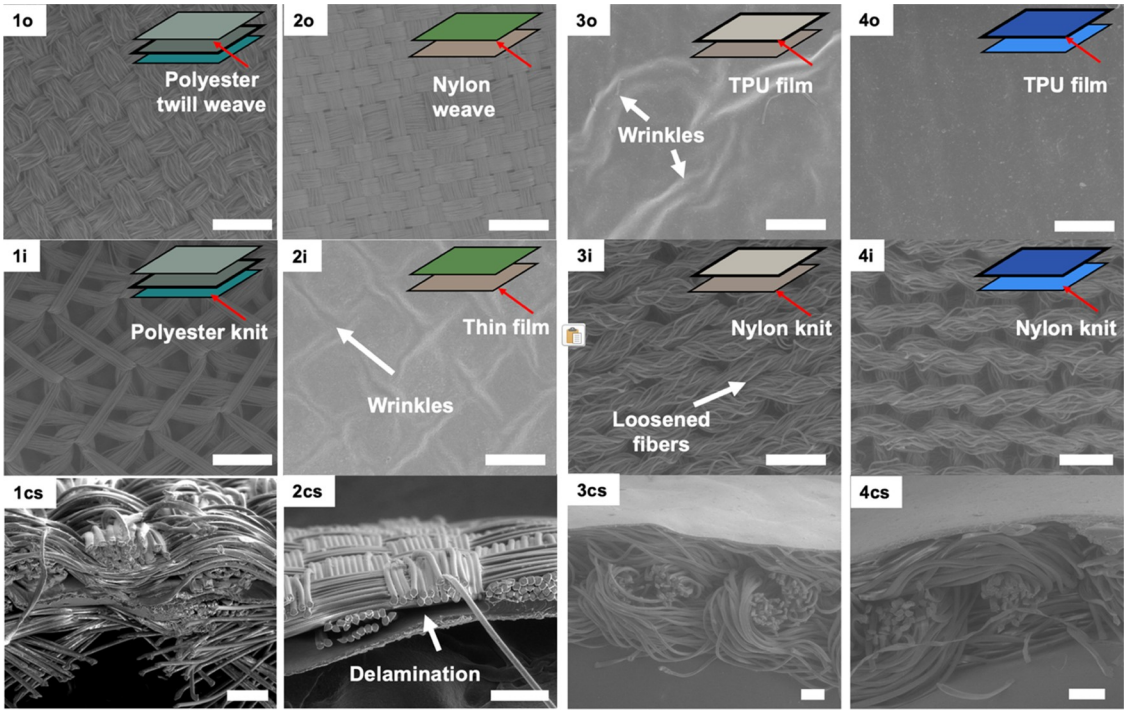

Figure 4. SEM images of the Janus fabrics were investigated after five washing cycles. Sample 1: a 3-layer laminate poly twill fabric with a middle ePTFE film layer. Sample 2: a 2.5-layer waterproof breathable ripstop fabric. Sample 3: a thermally laminated TPU fabric with a hydrophilic inner layer. Sample 4: a thermally laminated TPU fabric with a hydrophobic inner layer. The first row (o) shows the outer layer, the second row (i) shows the inner layer, and the (cs) third row (cs) shows the cross-sectional view of the fabric, with the inner layer on top and the outer layer at the bottom. Specific changes in fabric morphology, including wrinkles, loosened fibers, and delamination of layers from washing, are highlighted. Scale bars for (o, i): 500 μm and for (cs): 100 μm.

https://doi.org/10.1021/acsami.2c09544
ACS Appl. Mater. Interfaces 2022, 14, 32579−32589

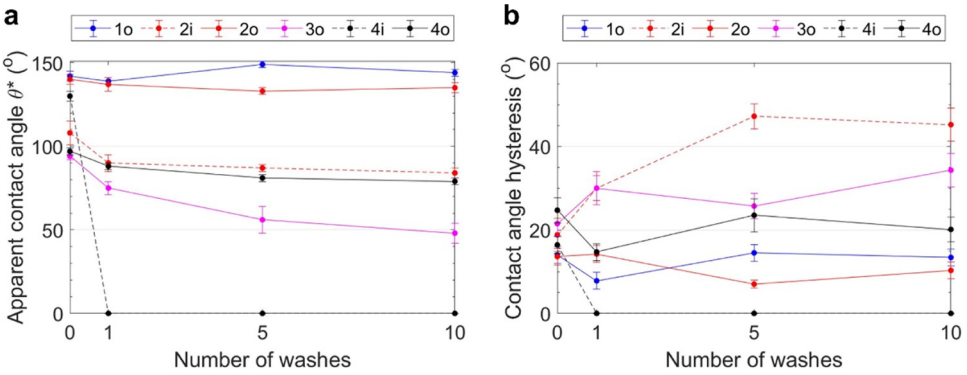

Figure 5. Wetting behavior of the Janus fabric samples after 0, 1, 5, and 10 washing cycles. (a) Apparent contact angle and (b) contact angle hysteresis. Samples **1i** and **3i** were excluded due to the complete wetting of the samples by water.

Table 4. FE at 0.3 μm of the Surgical Mask, N95 Respirator, and Janus Fabric Samples after 0, 1, 5, and 10 Wash Cycles Measured at a Face Velocity of 9.2 cm s^{-1}[a]

sample	original (%)	1 cycle (%)	5 cycle (%)	10 cycle (%)
1i (polyester knit)	48.99 ± 1.61	51.06 ± 2.60	50.52 ± 0.80	49.89 ± 0.73
1o (polyester twill weave)	31.23 ± 0.47	31.17 ± 2.27	32.65 ± 1.39	33.14± 2.70
2i (ePTFE film)	N/A	N/A	N/A	N/A
2o (nylon weave)	N/A	N/A	N/A	N/A
3i (nylon knit)	N/A	N/A	N/A	N/A
3o (TPU film)	63.26 ± 1.26	62.05 ± 1.81	63.86 ± 0.89	62.16 ± 1.07
4i (nylon knit)	N/A	N/A	N/A	N/A
4o (TPU film)	53.34 ± 1.53	55.90 ± 1.28	53.38 ± 2.02	52.68 ± 1.26
5 (surgical mask)	50.07 ± 0.18	32.73 ± 3.57	26.27 ± 0.66	25.77 ± 0.64
6 (N95 respirator)	98.16 ± 0.69	65.74 ± 1.33	63.47 ± 0.2	45.28 ± 1.54

[a]Some FE data is not available because the pressure difference generated at the interface is greater than the maximum value allowed by the SMPS.

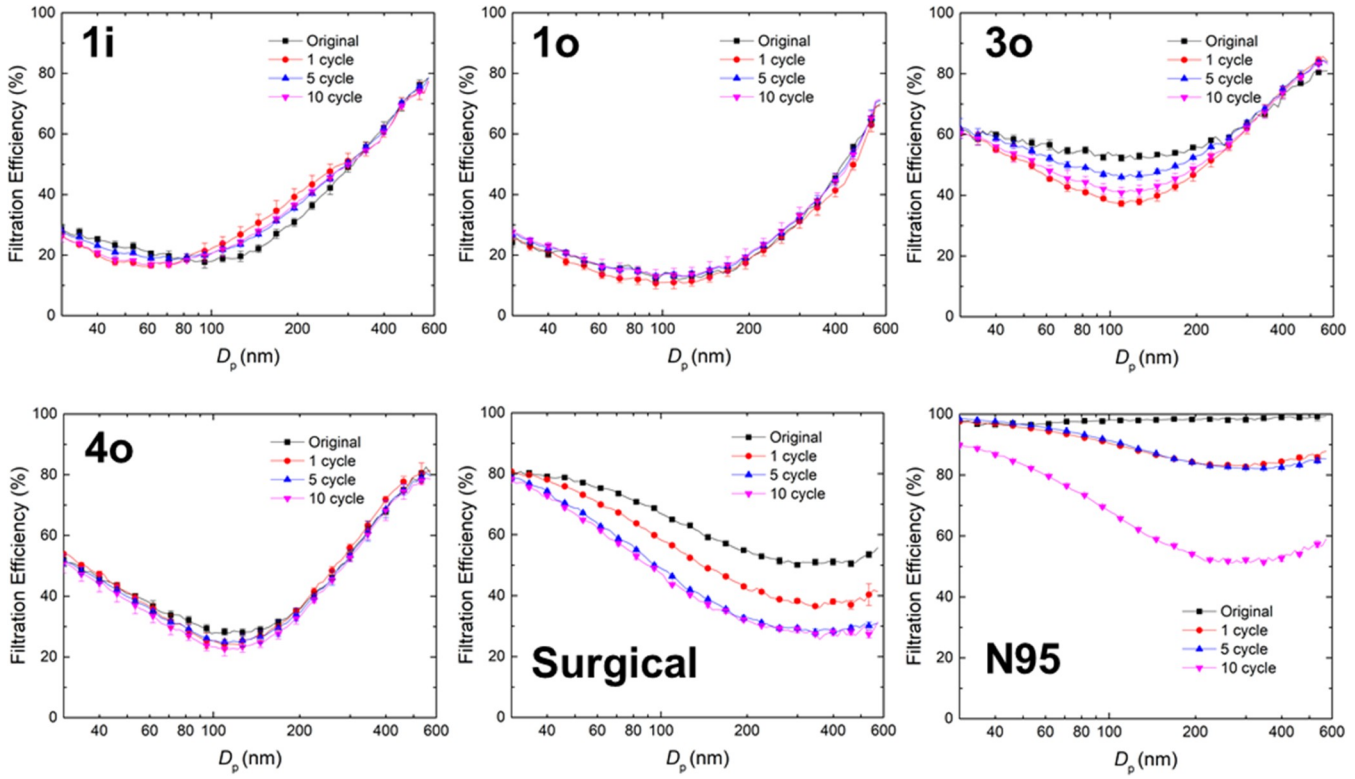

Figure 6. Size-dependent FE of the surgical mask, N95 respirator, and Janus fabric samples after 0, 1, 5, and 10 washing cycles at a face velocity of 9.2 cm s^{-1}.

https://doi.org/10.1021/acsami.2c09544
ACS Appl. Mater. Interfaces 2022, 14, 32579−32589

the wetting behaviors of the layers. Figure 5 shows changes in θ^* and CAH of the fabric layers after 1, 5, and 10 cycles of washing. In the outer layers, the more hydrophobic fabrics saw a general decrease in θ^* and an increase in CAH up to 10 washes, except **1o**, of which θ^* is almost not changed after 10 washes but CAH increases. In the inner layers, θ^* decreases and CAH increases after washes, including a complete loss of hydrophobicity in the **4i** nylon weave layer. **1i** and **3i** remained completely wetted after 10 cycles. **2i** and **2o** layers saw a much larger decrease in θ^* and increase in CAH compared to sample 1. **2i** loses its hydrophobicity, changing θ^* from 108 ± 7° (before wash) to 84 ± 3° after 10 washes and a CAH increase from 18.8 to 45.2°. The change in θ^* and CAH for **2o** was much less, retaining its hydrophobicity with a θ^* of 135 ± 3° and CAH < 15° even after 10 washes. The drop in θ^* on the **2i** layer was likely due to the entrapping of detergent on the surface since the morphology of the fibers remained nearly unchanged. After 10 washes, there was over a 20° drop in θ^*, from 94 ± 2° to 48 ± 6° for **3o** and from 97 ± 2° to 79 ± 2° for **4o**, while CAH remained over 20°. This loss of hydrophobicity would negatively impact the TPU film's ability to repel aerosols. **4i** with a hydrophobic nylon knit layer saw a complete loss of hydrophobicity after just one wash cycle, possibly caused by the removal of the hydrophobic coating on the woven fibers. The decrease in θ^* and the increase in CAH make aerosols more likely to penetrate through the fabric layers, thus diminishing their overall FE performance. **1o** and **2o** with a tightly woven outer layer fared the best among the Janus fabric layers in retaining its wetting behavior after 10 washes. The chemical compositions of the fabric samples were measured before and after the washing cycles by energy-dispersive X-ray spectroscopy (EDS) (Table S2). Although we did not see a clear correlation between the change in chemical compositions and the change in wetting behaviors, we observed the loss of nitrogen and increase of oxygen in all samples except fabric 1, which had no nitrogen but an increase of oxygen after washing.

Besides the characterization of fabric morphology and wetting behaviors, we evaluated the FE performance of the Janus fabric samples, surgical masks, and N95 respirators after 1, 5, and 10 washing cycles (see the summary in Table 4 and Figure 6). As seen in Figure 6, FE of samples **1i** and **1o** showed similar overall FE performance and size-dependent FE within error, even after 10 washing cycles, attributed to the nearly intact structural morphology. In the **3o** layer, the overall FE performance drops ∼10% and up to 15% for a 100 nm particle size. This can be attributed to the deterioration of the TPU film layers, allowing greater penetration of smaller particles through the fabric. The **4o** TPU film layer sees a smaller dip in the overall FE performance compared to the **3o** layer. In contrast, the overall FE of surgical masks decreases by >25% compared with the original one after 10 washing cycles, and in N95 respirators, the overall FE dropped significantly, >30%, after 10 washing cycles and from 98 to 51% at a 0.3 μm particle size after 10 washing cycles. These results are similar to those reported in the literature.[10] Washing not only loosens fibers in the nonwoven layers but also removes the electrostatic charges on fibers. Therefore, the nonwoven layers can only rely on mechanical interactions to filter out particles after cycles of washing. Since commercial Janus fabric layers can maintain their overall FE even after 10 washing cycles, they offer attractive alternatives to create effective, sustainable, and reusable fabric facemasks. Among the fabrics studied, sample 1 demonstrates excellent durability against washing, despite a lower overall FE performance in the submicron particle size range (FE overall = 25.64 ± 0.99%, FE at 0.3 μm = 48.99 ± 1.61%) and a higher pressure drop (ΔP = 3.26 ± 0.8 kPa) compared with other commercial Janus fabrics and surgical masks and N95 respirators.

CONCLUSIONS

Commercial fabrics with Janus-like behaviors are evaluated by their filtration performance, morphology, wetting behavior, and washing for the use of sustainable, durable, high-performance facemask materials. The selection of these fabrics for investigation is inspired by the design, composition, and functionality of athletic and rainwear, with its ability to repel water droplets while remaining breathable for long-term wear. Compared with prior work on evaluating commercial fabrics for easy-to-make facemasks, this study highlights the importance of material selections where the morphology and wetting behaviors of the fibers play important roles in breathability, filtration efficiency, and durability. Fabric layers that are hydrophobic in nature with small pores show the best FE performances due to their ability to intercept submicron particles, as well as to prevent liquid penetration and repel large droplets and aerosols. Layers with large pores are better for breathability. Tightly woven fabric layers and the hydrophobic nature of the fibers are critical for long-term durability to withstand mechanical abrasion and chemical alteration from washing cycles. We envision that our study will inspire the development of better Janus fabrics for facemasks and lead the additional investigation of the roles of lamination and adhesion of the fabric layers on filtration efficiency, breathability, and durability.

ASSOCIATED CONTENT

Supporting Information

The Supporting Information is available free of charge at https://pubs.acs.org/doi/10.1021/acsami.2c09544.

FE at 0.3 μm of surgical masks, N95 respirators, and Janus fabric samples; element compositions of the inner and outer layers of different fabrics before and after washing for five cycles; schematic of the filtration performance experimental setup; SEM images of the pristine surgical mask and N95 respirator samples before and after five washing cycles; comparison of FE of different brands of surgical masks, N95, and KN95 respirators; size-dependent FE of the surgical mask, N95 respirator, and Janus fabric samples; and size-dependent FE of the surgical mask, N95 respirator, and Janus fabric samples with wet aerosols at 20, 40, and 60% relative humidities (RHs) (PDF)

AUTHOR INFORMATION

Corresponding Author

Shu Yang − *Department of Materials Science and Engineering, University of Pennsylvania, Philadelphia, Pennsylvania 19104, United States;* orcid.org/0000-0001-8834-3320; Email: shuyang@seas.upenn.edu

Authors

Steven Cheng − *Department of Materials Science and Engineering, University of Pennsylvania, Philadelphia, Pennsylvania 19104, United States*

https://doi.org/10.1021/acsami.2c09544
ACS Appl. Mater. Interfaces 2022, 14, 32579−32589

Weixing Hao − *Department of Civil, Architectural and Environmental Engineering, Missouri University of Science and Technology, Rolla, Missouri 65409, United States*
Yuchen Wang − *Department of Materials Science and Engineering, University of Pennsylvania, Philadelphia, Pennsylvania 19104, United States;* orcid.org/0000-0002-6710-6710
Yang Wang − *Department of Civil, Architectural and Environmental Engineering, Missouri University of Science and Technology, Rolla, Missouri 65409, United States;* orcid.org/0000-0002-0543-0443

Complete contact information is available at: https://pubs.acs.org/10.1021/acsami.2c09544

Notes

The authors declare no competing financial interest.

■ ACKNOWLEDGMENTS

The authors acknowledge support from the National Science Foundation (NSF) through the PIRE program #OISE-1545884 and, in part, by Future Manufacturing Research Grant (FMRG), # CMMI-2037097. The authors also acknowledge the use of SEM supported by the NSF/Materials Research Science and Engineering Center (MRSEC) at the University of Pennsylvania, #DMR-1720530. Y.W. and W.H. are also partly supported by the NSF CBET grant, #CBET-2034198. Eric Sugalski is acknowledged for suggesting looking into the polyurethane laminate (PUL) fabric.

■ REFERENCES

(1) Morawska, L.; Cao, J. Airborne transmission of SARS-CoV-2: The world should face the reality. *Environ. Int.* **2020**, *139*, No. 105730.
(2) Adhikari, S. P.; Meng, S.; Wu, Y.-J.; Mao, Y.-P.; Ye, R.-X.; Wang, Q.-Z.; Sun, C.; Sylvia, S.; Rozelle, S.; Raat, H.; Zhou, H. Epidemiology, causes, clinical manifestation and diagnosis, prevention and control of coronavirus disease (COVID-19) during the early outbreak period: a scoping review. *Infect. Dis. Poverty* **2020**, *9*, No. 29.
(3) COVID-19 Decontamination and Reuse of Filtering Facepiece Respirators. www.cdc.gov/coronavirus/2019-ncov/hcp/ppe-strategy/decontamination-reuse-respirators.html (accessed June 2022).
(4) Wang, Y.; Deng, Z.; Shi, D. How effective is a mask in preventing COVID-19 infection? *Med. Devices Sens.* **2021**, *4*, No. e10163.
(5) Tang, S.; Mao, Y.; Jones, R. M.; Tan, Q.; Ji, J. S.; Li, N.; Shen, J.; Lv, Y.; Pan, L.; Ding, P.; et al. Aerosol transmission of SARS-CoV-2? Evidence, prevention and control. *Environ. Int.* **2020**, *144*, No. 106039.
(6) Konda, A.; Prakash, A.; Moss, G. A.; Schmoldt, M.; Grant, G. D.; Guha, S. Aerosol filtration efficiency of common fabrics used in respiratory cloth masks. *ACS Nano* **2020**, *14*, 6339−6347.
(7) Drewnick, F.; Pikmann, J.; Fachinger, F.; Moormann, L.; Sprang, F.; Borrmann, S. Aerosol filtration efficiency of household materials for homemade face masks: Influence of material properties, particle size, particle electrical charge, face velocity, and leaks. *Aerosol Sci. Technol.* **2021**, *55*, 63−79.
(8) Li, I.W.-s.; Fan, J. K.; Lai, A. C.; Lo, C. M. Home-made masks with filtration efficiency for nano-aerosols for community mitigation of COVID-19 pandemic. *Public Health* **2020**, *188*, 42−50.
(9) Kwong, L. H.; Wilson, R.; Kumar, S.; Crider, Y. S.; Reyes Sanchez, Y.; Rempel, D.; Pillarisetti, A. Review of the breathability and filtration efficiency of common household materials for face masks. *ACS Nano* **2021**, *15*, 5904−5924.
(10) Jung, H.; Kim, J. K.; Lee, S.; Lee, J.; Kim, J.; Tsai, P.; Yoon, C. Comparison of filtration efficiency and pressure drop in anti-yellow sand masks, quarantine masks, medical masks, general masks, and handkerchiefs. *Aerosol Air Qual. Res.* **2014**, *14*, 991−1002.
(11) Hao, W.; Parasch, A.; Williams, S.; Li, J.; Ma, H.; Burken, J.; Wang, Y. Filtration performances of non-medical materials as candidates for manufacturing facemasks and respirators. *Int. J. Hyg. Environ. Health* **2020**, *229*, No. 113582.
(12) Hao, W.; Xu, G.; Wang, Y. Factors influencing the filtration performance of homemade face masks. *J. Occup. Environ. Hyg.* **2021**, *18*, 128−138.
(13) Mueller, W.; Horwell, C. J.; Apsley, A.; Steinle, S.; McPherson, S.; Cherrie, J. W.; Galea, K. S. The effectiveness of respiratory protection worn by communities to protect from volcanic ash inhalation. Part I: Filtration efficiency tests. *Int. J. Hyg. Environ. Health* **2018**, *221*, 967−976.
(14) Hao, J.; Passos de Oliveira Santos, R.; Rutledge, G. C. Examination of nanoparticle filtration by filtering Facepiece respirators during the COVID-19 pandemic. *ACS Appl. Nano Mater.* **2021**, *4*, 3675−3685.
(15) Bhattacharjee, S.; Bahl, P.; De Silva, C.; Doolan, C.; Chughtai, A. A.; Heslop, D.; MacIntyre, C. R. Experimental evidence for the optimal design of a high-performing cloth mask. *ACS Biomater. Sci. Eng.* **2021**, *7*, 2791−2802.
(16) Pei, C.; Ou, Q.; Kim, S. C.; Chen, S.-C.; Pui, D. Y. Alternative face masks made of common materials for general public: Fractional filtration efficiency and breathability perspective. *Aerosol Air Qual. Res.* **2020**, *20*, 2581−2591.
(17) Radney, J. G.; Weaver, J. L.; Vicenzi, E. P.; Staymates, M. E.; Zangmeister, C. D. Filter inserts impact cloth mask performance against nano-to micro-sized particles. *ACS Nano* **2021**, *15*, 12860−12868.
(18) Zangmeister, C. D.; Radney, J. G.; Vicenzi, E. P.; Weaver, J. L. Filtration efficiencies of nanoscale aerosol by cloth mask materials used to slow the spread of SARS-CoV-2. *ACS Nano* **2020**, *14*, 9188−9200.
(19) Reutman, S. R.; Reponen, T.; Yermakov, M.; A Grinshpun, S. Homemade facemasks: particle filtration, breathability, fit, and other performance characteristics. *J. Occup. Environ. Hyg.* **2021**, *18*, 334−344.
(20) Zhao, M.; Liao, L.; Xiao, W.; Yu, X.; Wang, H.; Wang, Q.; Lin, Y. L.; Kilinc-Balci, F. S.; Price, A.; Chu, L.; et al. Household materials selection for homemade cloth face coverings and their filtration efficiency enhancement with triboelectric charging. *Nano Lett.* **2020**, *20*, 5544−5552.
(21) Rengasamy, S.; Eimer, B.; Shaffer, R. E. Simple respiratory protection—evaluation of the filtration performance of cloth masks and common fabric materials against 20−1000 nm size particles. *Ann. Occup. Environ. Hyg.* **2010**, *54*, 789−798.
(22) Dhanraj, D. I. A.; Choudhary, S.; Jammalamadaka, U.; Ballard, D. H.; Kumfer, B. M.; Dang, A. J.; Williams, B. J.; Meacham, K. W.; Axelbaum, R. L.; Biswas, P. Size-dependent filtration efficiency of alternative facemask filter materials. *Materials* **2021**, *14*, 1868.
(23) Hill, W. C.; Hull, M. S.; MacCuspie, R. I. Testing of commercial masks and respirators and cotton mask insert materials using SARS-CoV-2 virion-sized particulates: Comparison of ideal aerosol filtration efficiency versus fitted filtration efficiency. *Nano Lett.* **2020**, *20*, 7642−7647.
(24) Davies, A.; Thompson, K.-A.; Giri, K.; Kafatos, G.; Walker, J.; Bennett, A. Testing the efficacy of homemade masks: would they protect in an influenza pandemic? *Disaster Med. Public Health Prep.* **2013**, *7*, 413−418.
(25) Esposito, S.; Principi, N.; Leung, C. C.; Migliori, G. B. Universal use of face masks for success against COVID-19: evidence and implications for prevention policies. *Eur. Respir. J.* **2020**, *55*, No. 2001260.
(26) Melayil, K. R.; Mitra, S. K. Wetting, Adhesion, and Droplet Impact on Face Masks. *Langmuir* **2021**, *37*, 2810−2815.
(27) Emi, H.; Okuyama, K.; Yoshioka, N. Prediction of collection efficiency of aerosols by high-porosity fibrous filter. *J. Chem. Eng. Japan* **1973**, *6*, 349−354.

(28) Hinds, W. C. *Aerosol Technology: Properties, Behavior, and Measurement of Airborne Particles*, John Wiley & Sons, 1999.
(29) Lee, K. W.; Liu, B. Theoretical study of aerosol filtration by fibrous filters. *Aerosol Sci. Technol.* **1982**, *1*, 147−161.
(30) Aydin, O.; Emon, B.; Cheng, S.; Hong, L.; Chamorro, L. P.; Saif, M. T. A. Performance of fabrics for home-made masks against the spread of COVID-19 through droplets: A quantitative mechanistic study. *Extreme Mech. Lett.* **2020**, *40*, No. 100924.
(31) Liu, H.; Cao, C.; Huang, J.; Chen, Z.; Chen, G.; Lai, Y. Progress on particulate matter filtration technology: basic concepts, advanced materials, and performances. *Nanoscale* **2020**, *12*, 437−453.
(32) Liu, C.; Hsu, P.-C.; Lee, H.-W.; Ye, M.; Zheng, G.; Liu, N.; Li, W.; Cui, Y. Transparent air filter for high-efficiency PM2.5 capture. *Nat. Commun.* **2015**, *6*, No. 6205.
(33) Sun, Y.; Zhang, X.; Zhang, M.; Ge, M.; Wang, J.; Tang, Y.; Zhang, Y.; Mi, J.; Cai, W.; Lai, Y.; Feng, Y. Rational Design of Electrospun Nanofibers for Gas Purification: Principles, Opportunities, and Challenges. *Chem. Eng. J.* **2022**, *446*, No. 137099.
(34) Ji, X.; Huang, J.; Teng, L.; Li, S.; Li, X.; Cai, W.; Chen, Z.; Lai, Y. Advances in particulate matter filtration: materials, performance, and application. *Green Energy Environ.* **2022**, DOI: 10.1016/j.gee.2022.03.012.
(35) Zhang, R.; Liu, B.; Yang, A.; Zhu, Y.; Liu, C.; Zhou, G.; Sun, J.; Hsu, P.-C.; Zhao, W.; Lin, D.; et al. In situ investigation on the nanoscale capture and evolution of aerosols on nanofibers. *Nano Lett.* **2018**, *18*, 1130−1138.
(36) World Health Organization. Coronavirus disease (COVID-19): Masks https://www.who.int/emergencies/diseases/novel-coronavirus-2019/question-and-answers-hub/q-a-detail/coronavirus-disease-covid-19-masks (accessed June 2022).
(37) Kennedy, M. E.; Hollenbaugh, D. L., Jr. Fluoropolymer barrier material. U.S. Patent No. US7,521,010. 21: 2009.
(38) Weder, M. Performance of breathable rainwear materials with respect to protection, physiology, durability, and ecology. *J. Coat. Fabrics* **1997**, *27*, 146−168.
(39) Hsieh, Y.-L.; Yu, B. Liquid Wetting, Transport, and Retention Properties of Fibrous Assemblies: Part I: Water Wetting Properties of Woven Fabrics and Their Constituent Single Fibers. *Textile Res. J.* **1992**, *62*, 677−685.
(40) Xu, P.; Ma, X.; Zhao, X.; Fancey, K. S. Experimental investigation on performance of fabrics for indirect evaporative cooling applications. *Build. Environ.* **2016**, *110*, 104−114.
(41) Wilson, P. A.; Dallas, M. J. Diaper performance: maintenance of healthy skin. *Pediatr. Dermatol.* **1990**, *7*, 179−184.
(42) Yang, H. C.; Hou, J.; Chen, V.; Xu, Z. K. Janus membranes: exploring duality for advanced separation. *Angew. Chem., Int. Ed.* **2016**, *55*, 13398−13407.
(43) Wang, Z.; Liu, G.; Huang, S. In situ generated Janus fabrics for the rapid and efficient separation of oil from oil-in-water emulsions. *Angew. Chem., Int. Ed.* **2016**, *55*, 14610−14613.
(44) Gu, J.; Xiao, P.; Chen, J.; Zhang, J.; Huang, Y.; Chen, T. Janus polymer/carbon nanotube hybrid membranes for oil/water separation. *ACS Appl. Mater. Interfaces* **2014**, *6*, 16204−16209.
(45) Lim, H. S.; Park, S. H.; Koo, S. H.; Kwark, Y.-J.; Thomas, E. L.; Jeong, Y.; Cho, J. H. Superamphiphilic janus fabric. *Langmuir* **2010**, *26*, 19159−19162.
(46) You, J. B.; Yoo, Y.; Oh, M. S.; Im, S. G. Simple and reliable method to incorporate the Janus property onto arbitrary porous substrates. *ACS Appl. Mater. Interfaces* **2014**, *6*, 4005−4010.
(47) Li, L.; Zuo, Z.; Japuntich, D. A.; Pui, D. Y. Evaluation of filter media for particle number, surface area and mass penetrations. *Ann. Occup. Hyg.* **2012**, *56*, 581−594.
(48) Rengasamy, S.; Eimer, B. C.; Shaffer, R. E. Evaluation of the performance of the N95-companion: effects of filter penetration and comparison with other aerosol instruments. *J. Occup. Environ. Hyg.* **2012**, *9*, 417−426.
(49) Becquemin, M.; Swift, D.; Bouchikhi, A.; Roy, M.; Teillac, A. Particle deposition and resistance in the noses of adults and children. *Eur. Respir. J.* **1991**, *4*, 694−702.
(50) Grinshpun, S. A.; Haruta, H.; Eninger, R. M.; Reponen, T.; McKay, R. T.; Lee, S.-A. Performance of an N95 filtering facepiece particulate respirator and a surgical mask during human breathing: two pathways for particle penetration. *J. Occup. Environ. Hyg.* **2009**, *6*, 593−603.
(51) Jahan, I. Effect of fabric structure on the mechanical properties of woven fabrics. *Adv. Res. Text. Eng.* **2017**, *2*, 1018.
(52) Mikučionienė, D.; Čiukas, R.; Mickevičienė, A. The influence of knitting structure on mechanical properties of weft knitted fabrics. *Mater. Sci.* **2010**, *16*, 221−225.
(53) Thomas, Y. III. An essay on the cohesion of fluids. *Philos. Trans. R. Soc. London* **1805**, *95*, 65−87.
(54) Wenzel, R. N. Resistance of solid surfaces to wetting by water. *Ind. Eng. Chem.* **1936**, *28*, 988−994.
(55) Wenzel, R. N. Surface roughness and contact angle. *J. Phys. Chem. A* **1949**, *53*, 1466−1467.
(56) Cassie, A. B. D.; Baxter, S. Wettability of porous surfaces. *Trans. Faraday Soc.* **1944**, *40*, 546−551.
(57) Stechkina, I.; Kirsch, A.; Fuchs, N. Studies on fibrous aerosol filters—iv calculation of aerosol deposition in model filters in the range of maximum penetration. *Ann. Occup. Hyg.* **1969**, *12*, 1−8.
(58) Brown, R.; Wake, D. Air filtration by interception—theory and experiment. *J. Aerosol Sci.* **1991**, *22*, 181−186.